ICES CM 2009/C:06
Not be cited without prior reference to the authors

Combining hydrographical particles-tracking models with spatial analyses to evaluate spatial dynamics of cod larvae and 0-group in the Barents Sea

Manuel Hidalgo[1], Yvonne Gusdal[2], Gjert Endre Dingsør[3], Lorenzo Ciannelli[4], Dag Hjermann[1], Geir Ottersen[5], Leif Christian Stige[1], Ingerid Fossum[2], Arne Melsom[2], and Nils Christian Stenseth[1, 6]

[1] Centre for Ecological and Evolutionary Synthesis (CEES), Department of Biology, University of Olso, PO Box 1066 Blindern, 0316 Oslo. manuel.hidalgo@bio.uio.no; d.o.hjermann@bio.uio.no; l.c.stige@bio.uio.no; n.c.stenseth@bio.uio.no.
[2] Norwegian Meteorological Institute, N-0313 Oslo, Norway. yvonne.gusdal@met.no; arne.melsom@met.no.
[3] Institute of Marine Research, P.O. Box 1870 Nordnes, 5817 Bergen, Norway. gjerted@imr.no.
[4] College of Oceanic and Atmospheric Science, Oregon State University 104 COAS Admin Bldg, Corvallis, OR 97331-5503, United States. lciannel@coas.oregonstate.edu.
[5] Institute of Marine Research, Gaustadalleen 21, N-0349 Oslo, Norway. geir.ottersen@imr.no.
[6] Institute of Marine Research, Flødevigen Marine Research Station, 4817 His, Norway.

ABSTRACT

Recruitment ecology of cod has been an important focus within the framework of GLOBEC. A large part of this work focused on understanding the spatiotemporal component of cod populations. For the early pelagic life stages, studies based on an individual-based platform have provided highly valuable insights combining oceanographic, behavioural and modelling approaches. The spatial modelling of observational data often fails to include density-dependent covariates, which for early pelagic life stages, originate from the combination of circulation patterns and eggs coming from the spawning aggregations. We performed this task combining a hydrographical particle-tracking model with spatial statistical analyses to investigate the relative contribution of hydrographical variables on the spatial distribution of cod larvae in the Barents Sea under two short-term climatic regimes in the period 1986-1991. The cod larvae distribution is modelled using eggs drifting from the spawning aggregations in the Lofoten Islands. We found that inter-annual variability in the spatial aggregations of the spawners influenced the distribution of larvae drifted. We have also shown how the spatial distribution of passive-drifting larvae can change over the two regimes (1986-1988 and 1989-1991), being more upstream in cold periods. Though the currents pattern is the main hydrographical factor shaping the spatial distribution of larvae, the temperature modifies such distribution by affecting larvae survival. However, our study highlights the geographic extension of the temperature effect changed between warm and cold periods, with clear ecological implications in terms of growth and survival. This approach can be useful for other fish populations to further understand the underlying processes shaping the seascape of early life stages.

Keywords: Barents Sea cod, larvae, hydrographical particles-tracking models, spatial analyses.

Introduction

The response of marine populations to variations in climate forcing has been an important focus of the Global Ocean Ecosystems Dynamics programme (GLOBEC) (e.g., Ottersen et al. 2009). Part of this work focused on understanding the spatiotemporal component of cod populations and addressed to investigate patterns and mechanisms affecting fish abundance and survival over space focusing on species-environment and demographic interactions (e.g., Ciannelli et al. 2007). Studies combining oceanographic, behavioural, and modelling approaches (mainly on an individual-based platform) have also provided new insights into the spatial ecology of marine fishes in the framework of GLOBEC program (Fiksen et al. 2007). Besides these valuable bio-physical modelling advances, oceanographic modelling is commonly not coupled with statistical techniques when inter-annual and spatial variability of early life stages of fish are analysed. Ultimately, the distribution of early life stages of fish (i.e., eggs/larvae) depends on fecundity, abundance of spawners, oceanographic forcing (circulation pattern) on the particles, and spatial and temporal pattern of selective forces (e.g., size selective feeding or mortality). To our knowledge, no study has combined hydrographical particle-tracking modelling with statistical spatial analyses to model observational data including environmental covariates to further understand the underlying processes shaping the spatial distribution of early life stages of fish. This may be due to the difficulty of combining inter-annual variability of spawners' aggregations with the complex and variable advection patterns for larvae away from the spawning sites. This combination can provide the density-dependent variable on the spatial distribution of larvae. We performed these tasks for the early life stages of cod (*Gadus morhua*) in the Barents Sea system (Figura 1a).

The Arcto-Norwegian cod is the main top predator in the Barents Sea system. The majority of mature fish, from about six to seven years old, migrate to the spawning grounds around the Lofoten archipelago (in the centre of the blue box in Figure 1a). Timing and duration of spawning have been shown to be independent of varying temperature conditions and spreads from early March to middle May, reaching the maximum intensity during the first week of April (Ellertsen et al. 1989). Early life stages (i.e., eggs and larvae) are passively transported by the Norwegian Coastal Current (NCC) and the North Atlantic Current (NAC), and settle to the bottom in the Barents Sea around September (Ellertsen et al.1981, Bergstad et al. 1987). Several studies have shown that larval behaviour (vertical position in the water column) can affect larval drift routes as well as growth, which is temperature-dependent (Fiksen et al., 2007, Vikebø et al. 2005, 2007). However, these studies did not explicitly study the actual spatial distribution of fish larvae; either investigated possible mechanisms that may affect spatial distribution. Changes in the spatial pattern of survival under different climatic and demographic regimes were recently demonstrated for juveniles of Arcto-Norwegian cod (i.e., age-0, one year old fish, Ciannelli et al., 2007). However, to date, no study has examined whether selective mortality due to variable environmental conditions modify the spatial distribution at the larval stage, when maximum natural mortality is expected, or whether the distribution differs among different climatic scenarios.

We investigate distribution patterns of larvae that drift from the spawning habitats in the Lofoten archipelago and how these patterns are affected by spawner distribution, density-dependent mortality, and different environmental covariates of the larval habitat. Our approach is to compare the distribution of virtual particles (hereafter drifters), drifted from spawning sites using hydrodynamic models, with the observed distribution of larvae in July. To do that, we incorporate drifter abundance for each year as a covariate in the statistical

spatial analyses. The other covariates we study are temperature (affects growth of eggs/larvae directly, and may affect larvae survival indirectly through food availability, Ottersen and Stenseth 2001); salinity (can drive the vertical position in the water column, affecting feeding and horizontal displacement; Saborido-Rey et al. 2003, Vikebø et al. 2005); and convergence/divergence (related to mesoscale activity and the degree of retention, which slows down the horizontal transport of eggs and larvae Skarðhamar et al. 2007). The study spans several years (1986-1991), comprising years with low and high abundances of spawners and recruits (Dingsør et al. 2007) as well as two climatic regimes as shown by the North Atlantic Oscillation index (Hurrell et al. 1995). Abundance of recruits is in itself linked to sea temperature and the strength of inflow to the Barents Sea (Ottersen et al. 2002). We studied nonlinear threshold responses to the environment and density-dependent relationships that are common in species distribution data over contrasting climatic regimes (Ciannelli et al., 2007). By combining hydrodynamic models and statistical techniques we reproduce the spatiotemporal dynamics of cod larvae and investigate the environmental-induced selective forces shaping the spatial larvae distribution when effects of density-dependence are taken into account.

Methods

Biological data
Larvae abundance was obtained in yearly cruises carried out off Northern Norway and in the western Barents Sea in June-July from 1977 to 1991. A pelagic trawl was used for sampling from 50 m to surface (see Bjørke and Sundby 1986 and Helle and Pennington 1999 for details). Information on spawning aggregations was obtained from acoustic abundance estimates from annual spring surveys carried out from 1986 and onwards in the Lofoten Islands area (Figure 2a). The spatial information was digitized for the study period (1986-1991) from Raknes and Sunnanå (1986) and internal (unpublished) survey reports at the Institute of Marine Research, Bergen, Norway (Annon., 1987, 1988, 1989, 1990, 1991). Although haddock and coastal cod were also included in the acoustic estimates, Arcto-Norwegian cod were most abundant and the estimates are considered as representative for the spawning habitats of this species (Raknes and Sunnanå 1986). The Lofoten area were divided into three sub-areas (Vestfjorden, Yttersida and Nord, Figure 2a) based on Ellertsen et al. (1989) to summarize and compare the spatial information. For each sub-area the centre of gravity was calculated relative to the spawners' abundance and used as starting points for the release of particles (i.e., eggs) in the hydrodynamic particle-tracking model (see details below). The inter-annual changes in the centres of gravity between areas were analysed by pairwise Spearman correlations.

The ocean/sea ice model
Currents, sea temperature, and salinity were obtained from a coupled model system consisting of an ocean model (MI-POM) and an ice model (MI-IM). MI-POM is the Norwegian Meteorological Institutes version of the Princeton Ocean Model, which is a full three-dimensional, primitive equation and terrain-following (σ-coordinate) model (Engedahl 1995, Engedahl et al. 2001). The MI-IM model is described by Røed and Debernard (2004). The coupled model system had a nested set-up as illustrated Melson and Fossum (2009). The coarse grid covers the Arctic Sea and the North Atlantic Ocean, with a resolution of 20 km (hereafter referred as the Arctic sea model). The fine grid within this has a mesh size of 4 km with 21 σ-layers, and covers the Barents Sea and most of the Norwegian Sea (the inner black square in Figure 1).

The Arctic sea model was initialized January 1, 1981 with monthly mean climatological values of hydrography, currents, and sea surface elevation. Initial fields for the ice model were specified with a 2 m ice thickness, 0 ice velocity and 75% ice concentration where the ocean temperature in the climatological data was 0°C or below. At the open boundary the physical oceanographic model was relaxed towards the climatology documented by Engedahl et al. (1997, 1998), and the ice was only allowed to drift out of the model domain. No tidal forcing was included. For river runoff and Baltic outflow, the climatological values and the method described by Martinsen et al. (1992) were used. The simulation was performed for the years 1981-1995 with atmospheric forcing fields from the ERA40 dataset obtained from the European Center of Medium-Range Weather Forecasts (ECMWF, http://ecmwf.com/). Assimilation of sea surface temperature and ice concentration was applied with a slightly modified version of the nudging method documented by Albretsen and Burud (2006).

The fine grid 4 km mesh size model was initialized January 1, 1984, by interpolating the corresponding simulated fields from the Arctic sea model onto its mesh. At the lateral boundaries tidal forcing (8 constituents) was added to the results for sea surface height from the coarse grid simulation. The model was ramped up for 1984 and 1985 using the atmospheric and freshwater forcing as described above, as well as assimilation of sea surface temperature and ice concentration. The resulting fields for January 1, 1986, were then used as initial conditions for simulating the period from 1986 to 1995.

Since the ocean circulation is a non-deterministic response to the atmospheric forcing, a ten-member ocean circulation ensemble has been run, where each ensemble only differ in the atmospheric forcing. The ensemble is constructed by using forcing fields from the ten-day forecast produced twice a day at ECMWF. The atmospheric forcing for the first ensemble member is created by extracting all the 12 hours prognoses data, and collects them in one atmospheric forcing file. The second ensemble consists of all the 24 hours forecast while the third consists of all the 36 hours forecast and so on. Due to limitations in available computer time, the ensemble is restricted to 10 members and only the five first days of the atmospheric forecast are used. More detailed information about the validation of the ocean model ensemble for the Barents Sea and the northeastern Nordic Seas can be found in Melson and Fossum (2009). An averaged over the ten ensemble members and the period June 24 to July 27 at 10 m depth was calculated for all the environmental variables used as covariates in the spatial statistical analyses (see *Statistical spatial analyses* hereafter). For salinity and temperature, an averaged field per day was firstly calculated for the ten ensemble members, and the average over the two weeks was computed afterwards. Convergence/divergence was calculated as a variable proxy of potential retention activity in areas with higher vertical activity. Convergence/divergence is also a proxy of the eddy activity and has been calculated directly from the velocity field with the function:

$$div\,\vec{v} = \nabla \bullet \vec{v} = \frac{\delta u}{\delta x} + \frac{\delta v}{\delta y}$$

where $\nabla = \vec{i}\,\frac{\delta}{\delta x} + \vec{j}\,\frac{\delta}{\delta y}$, $\vec{v} = \vec{i}\,u + \vec{j}v$ and u, v is the x- and y- component of the current field. Because, convergence/divergence values can change at small spatial scale very rapidly over a

short time period (i.e., hours) we used the standard deviation over the aforementioned two weeks as the best proxy of vertical activity in the period studied.

The hydrodynamic particle-tracking model and initialization of drifters
The egg/larvae drift is computed based on a semi-Lagrange advection model forced by currents from the ensemble members. The drift computations which are based on ocean circulation model results are referred to as 'the hydrodynamical particle-tracking model' elsewhere. Due to the fine mesh size of 4 km for the model, high resolution current fields are simulated resolving ocean eddies. However, even though the trajectories are computed based on results from an eddy-permitting model, there are processes at finer scales that are not resolved by the model. This may lead to an underestimation in the spread of particles. These processes have been parameterized by adding Gaussian noise to the model results with a velocity $u^{adv} = u^{mdl} + u'$, where u^{mdl} is the velocity component from the model results and $u' \sim N(0, u_0^2)$ is the Gaussian noise with a standard deviation of u_0. In order to estimate the velocity scale u_0, the simulated dispersion is compared with released surface drifters and u_0 is tuned until the best correspondence between simulations and observations is found. Due to lack of drifters for the simulated years, drifters for the year 2007 have been used to describe the dispersion in the area. A good match was achieved with a velocity scale of 0.005 m/s (Melsom and Gusdal 2009).

We calculated the egg/larvae drifted by accounting for the different spawning sub-areas around the Lofoten archipelago, the timing of spawning, the depth, and the intra-annual variation of spawners' abundance. For each sub-area (Vestfjorden, Yttersida and Nord) and for each year, 15000 particles were released in the sub-area's centre of gravity (Figure 2). To account for the spawning period provided by Ellertsen et al. 1989, particles were released March 15, April 1 and April 15. In total, 135000 particles were released for each year, drifting for 90 days, and standardized afterwards based on assumptions from findings obtained from Ellertsen et al. (1989). Firstly, we assumed that depth distribution can be summarized in 75% of the particles drifted at 10 m depth and 25% at 20 m depth (Ellertsen et al. 1989). Our model is two-dimensional and disregards vertical movements, but there is little evidence of diel migration of larval and pelagic juvenile cod in this region, probably because there is 24-h daylight during summer (Vikebø et al. 2005). Secondly, we assumed that 68% of the eggs were released April 1, and 16% were both released March 15 and April 15 (Ellertsen et al. 1989). Thirdly, we took into account the relative abundance of spawners in each sub-area within each year (Figure 3). Finally, the inter-annual variation of spawner abundance based on the assessment outputs was taken into account for the final standardized distributions (Figure 3).

Statistical analysis of cod larvae distribution
We investigated the underlying processes which determine seascape of cod larvae under the potential occurrence of different climatic scenarios. Prior to modeling, the natural logarithm of observed larvae abundances (plus a constant, k = 0.5) were interpolated by means of ordinary kriging over a regular grid (Planque et al. 2007). To allow direct comparison of the different types of data we used a standardized grid for the kriging, the hydrographic, and particle-tracking models. Kriged data for cod larvae were regressed against co-located covariates using a generalized additive modeling (GAM, Hastie and Tibshirani, 1990). The values for the covariates were taken from the model output at 10 m depth (see *The ocean/sea ice model* section for details). We used two types of GAM formulations: (i) pure additive,

assuming that the effect of the covariates is stationary, that is the functional form of the effect does not change over years, and (ii) threshold (nonadditive), to test the hypothesis that the effect of a covariate changes in relation to an external threshold variable (e.g., different climatic regime). The additive formulation used is:

$$L_{t,(x,y)} = year + s(x,y) + f[D_{(x,y)}] + g[T_{(x,y)}] + h[S_{(x,y)}] + j[CD_{(x,y)}] + \varepsilon_{(x,y)}$$

where *year* was taken into account as a fixed factor to account for the mean level of each year, *s* is a two-dimensional non parametric smoothing function (thin plate regression spline, Wood 2003, with maximally 27 degrees of freedom [28 knots]), *f*, *g*, *h*, and *j* are one-dimensional non parametric smoothing functions (cubic splines, Wood 2004, with maximally 3 degrees of freedom [4 knots]), *x* and *y* are the location in the grid defined (Figure 1a), D is the natural logarithm of the density of drifters (plus a constant, k = 0.5) output from particle-tracking model, T is the temperature, S is the salinity, CD is the standard deviation of a convergence/divergence values over two weeks, and $\varepsilon_{(x,y)}$ is a normally distributed error term.

To test the hypothesis of different effect of covariates under different climatic regimes we implement the threshold non-additive formulation (TGAM, Ciannelli et al. 2004, 2007). TGAM is a semi-parametric regression where the shape of the exploratory function may change according to whether an external covariate is below or above a threshold value. The TGAM formulation becomes:

$$L_{t,(x,y)} = year + \varepsilon_{(x,y)} + \begin{cases} s_1(x,y) + f_1[D_{(x,y)}] + g_1[T_{(x,y)}] + h_1[S_{(x,y)}] + j_1[CD_{(x,y)}] & if \quad NAO_t \le n \\ s_2(x,y) + f_2[D_{(x,y)}] + g_2[T_{(x,y)}] + h_2[S_{(x,y)}] + j_2[CD_{(x,y)}] & if \quad NAO_t > n \end{cases}$$

We ran TGAM formulation applying NAO index threshold, *n*, on each of the covariates explored (location effect, drifters, temperature, salinity and presence of convergence/divergence activity). The best model, GAM or TGAM, was determined according to the (genuine) cross validation (CV, a random sample of 10% of the data was used for these calculations; see Ciannelli et al. 2004 for details). Low values indicate the best model compromise between model complexities and fit to the observed data. The residuals did not show temporal dependency but were spatially correlated. This results in an overestimation of the significance level of the covariates, and thus invalidates the standard *p*-values (Llope et al. 2009). We computed a non-parametric bootstrap to get an accurate estimate of *p*-values and confidence intervals of covariates. All the models, calculations and data pre-processing were coded in R (version 2.6.1; R Development Core Team 2007). The packages used were mgcv (Wood 2006), tgam (Ciannelli et al. 2004), fields (Furrer et al.2009) and RColorBrewer (Neuwirth 2007).

Results

Spawning aggregations

The spawning aggregations are confined to three main sub-areas around the Lofoten archipelago; Vestfjorden, Yttersida, and Nord (Figure 2). Both spatial distribution (i.e., centres of gravity) and abundance of su-bareas varied among years (Figure 2 and 3). Centres of gravity were generally allocated more offshore in Yttersida and Nord in the period from 1987 to 1989 compared to 1986, 1990 and 1991. Additionally, centres of gravity were in the outer area of Vestfjorden from 1987 to 1989 and 1991. Pairwise correlation among centres of

gravity showed certain consistency in the spatial-temporal variation. X-axis position was highly and positively correlated between Vestfjorden and Yttersida ($r = 0.92$, $P < 0.05$) while Y-axis position were negatively correlated between Nord and Vestfjorden ($r = -0.74$, $P < 0.05$).

The relative contribution of each sub-area to the annual abundance in Lofoten Islands also showed inter-annual variation (Figure 3). With the exception of 1987 and 1991, the contribution of the different sub-areas was quite constant (around 55% in Yttersida, 25% in Vestfjorden and 20% in Nord). In 1987, the contribution of Nord sub-area increased to 51%. In 1991, a year with increased spawner abundance, the contribution of Nord sub-area decreased to 6% and Vestforden and Yttersida both contributed around 47%. The interannual variation of temperature in the Lofoten grounds in March-April shows a clear increasing trend in this period (Figure 3).

Particle-tracking model
Model particles were released at the centres of gravity of the three spawning grounds in Lofoten around spawning time (April 1). They were transported by the circulation model, and resulting larvae distribution were then recorded at the time of the larval survey (around July 1), i.e. after 90 days of drift (Figure 4). If we do not take into account the varying abundance and distribution of the spawning stock, the distribution after 90 days combining contribution of the three spawners grounds shows the existing inter-annual and spatial variation in the spreading of particles only due to interannual variation in current patterns (Figure 4a). Figure 4b shows the distribution of drifters when the relative contribution of each sub-area is taken into account. Having taken into account total spawners' abundance, the high spread of drifters in 1987 is still observed yet the distribution in 1991 extended largely beyond the other years (Figure 4b). The distribution of drifters obtained accounting the total spawners' abundance (Figure 4b) was used as proxy of potential larvae distribution in the statistical modelling described below.

Spatial analyses
We analysed survey data on the distribution of larvae (Figure 5) using additive or non-additive models with one to five covariates (Figure 6a, 6b. 6c). The best model obtained showed non-additive threshold effects (TGAM, Figure 7) for the temperature and spatial pattern while additive for salinity, drifters and convergence/divergence activity and being year factor also significant ($p < 0.05$, Figure 7a). However, the non-parametric bootstrap indicated that salinity was not significant ($P = 0.18$). The final model shows the spatial pattern for low NAO regimes (<1, 1986-1988) ($P < 0.05$, Figure 7b) showed different functional form compared to high NAO regime (>1, 1989-1991) ($P < 0.05$, Figure 7c). Temperature effect for low and high NAO regimes showed also different functional forms in the effects (both additive effects $P < 0.05$, Figure 7d). Drifters effect showed a significant dome-shaped effect ($P < 0.05$, Figure 7e). Convergence / divergence activity effect was marginally significant ($P = 0.073$, Figure 7f). The final model explained 84% of the variance.

Discussion

Spatial dynamics of species-environment interactions in the early life fish stages are complex due to the drift forcing of the ocean currents. Disentangling the relative effects of biotic and abiotic factors influencing the spatial distribution of fish larvae is a major goal for fisheries ecologists and managers (Ciannelli et al. 2008), and more recently for the ecosystem-based

approach to fisheries (Le Quesne et al. 2008) and its social services (Kock et al. 2009). The methodology we provided in this study helps to integrate biological spawners' information, advective current patterns and environmental information of the larvae habitat to statistically model the spatial distribution of cod larvae in the Barents Sea.

The spatiotemporal variation of the spawning aggregations has been shown for the Barents Sea cod over large temporal scale (Sundby and Nakken 2008), with potential implications on the offspring fitness (Jørgensen et al. 2008). Sundby and Nakken (2008) showed inter-decadal displacements of cod spawning aggregations between cold and warm periods on longer (multidecadal) time scales. They considered the period from mid-1980s to be one of the warm periods, with the Lofoten grounds as the most important area for the spawners' aggregations. However, our results show that, within the Lofoten area, the inter-annual variation in the centres of gravity is consistent between sub-areas and indicates a certain spatial synchrony in the aggregation patterns. The interannual variation of temperature in the Lofoten grounds in spring shows an increasing trend (Figure 3) consistent with a change in the North Atlantic climatic regimes (Ottersen et al 2002). The phenology of *Calanus finmarchicus* spawning in this area is related to spring temperature (Ellertsen et al. 1989). This could lead to a match-mismatch situation between first-feeding cod larvae and their prey, resulting in a dome-shaped relationship between spring temperature in Lofoten and larvae survival. However, the short temporal scale of our study does not allow exploring this potential effect. The relative contribution of each sub-area to the annual abundance in Lofoten Islands also showed inter-annual variation (Figure 3). The combination of spatial location and relative abundance of spawners can have a potential effect on the seascape of early life stages of cod as we discuss hereafter. Since the spawning phenology is consistent between years, being determined by the seasonal light cycle (Sundby and Nakken 2008), the location and abundance of spawners will be the main sources of variance for the initial distribution of eggs that will be dispersed by the currents. However, the size structure and physiological condition of the mature stock can affect the survival of their offspring (Jørgensen et al. 2008). Larger and older spawners have higher fecundity and are better-conditioned, providing better fitness gain (i.e., increased survival) to their offspring (Jørgensen et al. 2008).

Model particles released at the spawning grounds in Lofoten and transported by the circulation model around 90 days were compiled in a unique larvae distribution per year (Figure 4). Our results evidenced the importance of combining abundance and distribution of mature individuals in the spawners grounds with the circulation pattern. An extreme example of the importance of combining this biological and the oceanographic information is 1987, when the higher contribution of spawners at sub-area Nord compared to other years (Figure 3) could facilitate a more extensive spreading of particles in the Barents Sea (Figure 4a). However, the sudden changes in spawners' abundance and distribution in 1991 (Figure 3) was the most important driver of change in the drifters' distribution in the studied period (Figure 4b). This approach can be improved, for instance using three-dimensional trajectory models to account for vertical movement, including size-structure information of the spawners (as discussed previously), or accounting for survival during the first weeks of life. However, the spatial distribution of drifters obtained by the particle-tracking model used in this study is comparable with results obtained by Vikebø et al. (2005), yet that study let the particles drift much longer (for five months, to the juvenile (0-group) stage). The distribution of drifters obtained accounting the total spawners' abundance (Figure 4b) let us to study density-dependent mortality processes shaping the seascape of larvae as we discuss hereafter.

The annual mean levels of larvae abundance (Figure 7a) show an increasing trend consistent with the inter-annual variation of spawners abundance (Figure 3). However, 1987 represented an exception in this trend showing as high values as in 1990 and 1991. Higher abundance of spawners in the Nord sub-area in 1987 compared to other years could result in a facilitation of eggs spreading by currents. This is evidence of the importance of including the effect of the spatial distribution of spawners in the particles drifting by currents. In our study, the relationship between drifters' abundance and observed larval abundance is asymptotic (Figure 7e). High values of drifters close to the coast are not translated in higher presence of larvae. Lower survival of early life stages very close to the coast is likely related to the stranding of eggs onto the coast and higher predation in coastal areas, although potential retention of eggs in fjords and higher mortality due to a density-dependent effect should not be disregarded. A potential bias might be attributed to the particle-tracking model (i.e., an overestimation of drifters in coastal areas due to bias in the current fields). However, our results are consistent with other studies applying different ocean models (Vikebø et al. 2005, 2007). Vikebø et al. 2005 showed that the spatial transport of eggs and larvae is depth-dependent. Above 10 m depth, the Norwegian Coastal Current (NCC) retains almost all the pelagic and passive-drifting stages close to the coast. Between 20 m and 30 m depth, eggs and larvae are mainly advected northwards by the North Atlantic Current (NAC) (Vikebø et al. 2005). Inter-annual variation in the vertical distribution of eggs is not included in our model, yet it could potentially occur; Sundby (1983) suggested that eggs are mixed deeper in the water column during windy conditions (related to warm climatic), while during calm conditions (cold periods) eggs are found in the upper mixed layer.

Having accounted for drifter abundance, (i.e., the effect of spawner distribution and larval advection), the model captures the potential effect of the other covariates on the larvae survival. The more relevant result is the different contribution of temperature and the spatial component to the larvae distribution under two short-term climatic regimes. Based on findings of different studies, we could expect higher abundance in warm periods because high inflow of zooplankton-rich Atlantic water is related to high temperatures (Dalpadado et al. 2003), in turn increasing larvae survival due to food availability (Ottersen and Stenseth 2001, Vikebø et al. 2005, 2007). However, our analysis showed that during warm periods, high abundances of larvae were found in temperatures around 9.5 ^{o}C, while in cold periods high abundances were found in temperatures above 10 ^{o}C. During cold periods, high larvae abundances were closely related to the warm core of the Atlantic water flowing northward. In contrast, the distribution of larvae in warm periods was more even and a high number of larvae were found in intermediate temperatures. Additionally, warm periods are often characterized by higher Atlantic inflow and a stronger NAC that can transport a high number of larvae far north and east, where there are lower temperatures (see for instance larvae distribution in 1990 and 1991 in Figure 5). This could lead to ecological implications in terms of survival, life history traits (i.e., growth), and underlying combined effects. Larvae growth is highly temperature-dependent (e.g. Folkvord 2005) and consequently the spatial location of drifting larvae will lead to the spatial variation of length for the subsequent early-life stages.

The spatial distribution of larvae showed clear and significant differences between regimes, being south-western in the period 1986-1988 (NAO < 1, cold period) and north-eastern in the period 1989-1991 (NAO > 1, warm period) (Figure 7b and 7c). Note that these are differences that remain after taking local temperature into account. The south-western distribution of larvae could initially be explained by a reduction in transport during cold periods (Ottersen et al. 2002; Vikebø et al. 2007). However, convergence/divergence activity

(Figure 7f) occurring in the most southward part of the shallow bank in the Barents Sea is most likely affecting the observed larvae distribution. This area with higher convergence/divergence activity occurs when NAC is deflected northwards and the NCC spreads out from the coast (Figure 8), developing a front between the water masses as demonstrated by the opposed correlation between salinity and temperature (Figure 8). This is an area with eventual occurrence of convergent eddies of low salinity and high temperature that increase the concentration of phytoplankton and zooplankton (Skarðhamar et al. 2007). Convergence/divergence activity in this area could probably slow down the northward transport of larvae and reinforce the southern distribution observed in cold periods. However, this covariate had a small and marginally significant effect on larval abundance (Figure 7f) due to a daily variability which makes it difficult to obtain spatially explicit information representative for each year. Spatial heterogeneity in the correlation between salinity and temperature (Figure 8) and earlier studies (Saborido-Rey et al. 2003, Vikerbø et al. 2005, see Introduction) justified the inclusion of salinity in the models, yet it turned out not significant in the model.

Conclusions

In summary, we provide a methodological framework to include spawners' abundance, and distribution as well as advection patterns in spatial analyses of pelagic early life stages of marine fish, combining quantitative information of spawner aggregations with particles-tracking based on results from a hydrodynamic model. Worth noticing is that the inter-annual variation in the spatial distribution of spawners within the Lofoten area can affect the spread of larvae into the Barents Sea. We have also shown how the spatial distribution of passive-drifting larvae can change over two short-term climatic regimes. Though the currents pattern is the main hydrographical factor shaping the spatial distribution of larvae, the temperature modifies such distribution by affecting larvae survival. However, our study highlights that the geographic extension of the temperature effect changed over the two studied climatic regimes, with clear ecological implications in terms of growth and survival. Early life stages of marine fish experience different environmental conditions throughout their distribution range. The procedure applied in this study shows a straightforward way to extract large scale ecological patterns from an observational dataset and will contribute to the understanding of the spatiotemporal variability of pelagic early life stages of marine fish under highly alternating climatic scenarios.

Literature cited

Anonymous (1987) *Intern toktrapport: Skreitokt i Lofoten*. Institute of Marine Research, Bergen, Norway (In Norwegian).

Anonymous (1988) *Intern toktrapport: Skreitokt i Lofoten*. Institute of Marine Research, Bergen, Norway (In Norwegian).

Anonymous (1989) *Intern toktrapport: Skreitokt i Lofoten*. Institute of Marine Research, Bergen, Norway (In Norwegian).

Anonymous (1990) *Intern toktrapport: Skreitokt i Lofoten.* Institute of Marine Research, Bergen, Norway (In Norwegian).

Anonymous (1991) *Intern toktrapport: Skreitokt i Lofoten.* Institute of Marine Research, Bergen, Norway (In Norwegian).

Albretsen J, Burud I (2006) Assimilation of sea surface temperature and sea ice concentration in a coupled sea ice and ocean model, in *European Operational Oceanography: Present and Future. Proceedings of the 4th International Conference on EuroGOOS.,* edited by H.

Dahlin, C. Flemming, P. Merchand, and S. E. Petersson, pp. 661-666, Brest, France.

Bjørke H, Sundby S (1986) Abundance indices and distribution of post larvae and 0-group cod. In: The Effect of Oceanographic Conditions on Distribution, and Population Dynamics of Commercial Fish Stocks in the Barents Sea—Loeng H., ed. (1986) Proceedings of the third Soviet-Norwegian Symposium in Murmansk, 26–30 May 1986. Bergen: Institute of Marine Research. 127–144. 250.

Ciannelli L, Chan KS, Bailey KM, Stenseth NC (2004) Nonadditive effects of the environment on the survival of a large marine fish population. *Ecology* 85: 3418–3427.

Ciannelli L, Dingsør GE, Bogstad B, Ottersen G, Chan KS, Gjøsæter H, Stiansen JE, Stenseth NC (2007) Spatial anatomy of species survival: Effects of predation and climate-driven environmental variability. *Ecology* 88: 635-646.

Ciannelli L, Fauchald P, Chan KS, Agostini VN, Dingsør GE (2008) Spatial fisheries ecology: Recent progress and future prospects. *J Mar Sys* 71: 223-236.

Dalpadado P, Ingvaldsen R, Hassel A (2003) Zooplankton biomass variation in relation to climatic conditions in the Barents Sea. *Polar Biol* 26: 233–241.

Dingsør GE., Ciannelli L, Chan KS, Ottersen G, Stenseth NS (2007) Density dependence and density independence during the early life stages of four marine fish stocks. *Ecology* 88:625–634.

Ellertsen B, Fossum P, Solemdal P, Sundby S (1989) Relation between temperature and survival of eggs and first feeding larvae of northeast Arctic cod (*Gadus morhua* L.). *Rapports et Proces-verbaux des Reunions Conseil International pour l'Exploration de la Mer* 191:209–219.

Ellertsen B, Moksness E, Solemdal P, Tilseth S, Westgård T, Øiestad V (1981) Feeding and vertical distribution of cod larvae in relation to availability of prey organisms. *Rapports et Proces-verbaux des Reunions Conseil International pour l'Exploration de la Mer* 178: 45–57.

Engedahl H (1995) Implementation of the Princeton ocean model (POM/ECOM-3D) at the Norwegian Meteorological Institute (DNMI). *Research Report 5,* Norwegian Meteorological Institute, Oslo, Norway.

Engedahl H, Eriksrød G, Ulstad C, Ådlandsvik B (1997) Climatological oceanographic archives covering the Nordic Seas and the Arctic Ocean with adjacent waters. *Research Report 59,* Norwegian Meteorological Institue, Oslo, Norway.

Engedahl H, Ådlandsvik B, Martinsen E (1998) Production of monthly mean climatological archives for the Nordic Seas. *J Mar Sys* 14*:* 1-26.

Engedahl H, Lunde A, Melsom A, Shi XB (2001) New schemes for vertical mixing in MI-POM and MICOM. *Research Report 118*, Norwegian Meteorological Institute, Oslo, Norway.

Folkvord A (2005) Comparison of size-at-age of larval Atlantic cod (*Gadus morhua*) from different populations based on size- and temperature-dependent growth models. *Can J Fish Aquat Sci* 62: 1037–1052.

Furrer R, Nychka D, Sain S (2009) Tools for spatial data. R-package version 5.02 .Available from: http://www.image.ucar.edu/Software/Fields.

Fiksen Ø, Jørgensen C, Kristiansen T, Vikebø F, Huse G (2007) Linking behavioural ecology and oceanography: larval behaviour determines growth, mortality and dispersal. *Mar Ecol Prog Ser* 347: 195-205.

Galindo HM, Olson DB, Palumbi SR (2006) Seascape genetics: A coupled oceanographic-genetic model predicts population structure of Caribbean corals. *Curr Biol* 16 (16): 1622-1626.

Koch EW, Barbier EB, Silliman BR, Reed DJ, Perillo GME, Hacker SD, Granek EF,

Primavera JH, Muthiga N, Polasky S, Halpern BS, Kennedy CJ, Kappel CV, Wolanski E (2009) Non-linearity in ecosystem services: temporal and spatial variability in coastal protection. *Front Ecol Environ* 7(1): 29-37.

Hastie TJ, Tibshirani RJ (1990) Generalized additive models. Chapman and Hall, London, UK.

Hurrell JW (1995) Decadal trends in the North Atlantic Oscillation: Regional temperatures and precipitation. *Science* 169: 676–679.

Jørgensen C, Dunlop ES, Opdal AF, Fiksen Ø (2008) The evolution of spawning migrations: state dependence and fishing-induced changes. *Ecology* 89 (12): 3436-3448.

Le Quesne WJF, Arreguin-Sánchez, F., Albanez-Lucero M, Cheng H-Q, Cruz VH, Daskalov G, Ding H, González-Rodríguez E, Heymans JJ, Jiang H, Lercari D, López-Ferreira C, López-Rocha JA, Mackinson S, Pinnegar JK, Polunin NVC, Wu J, Xu H-G, Zetina-Rejon MJ (2008) Analysing ecosystem effects of selected marine protected areas with Ecospace spatial ecosystem models. *University of British Columbia Fisheries Centre Research Reports*, 16 (2): 1-67.

Llope M, Chan KS, Ciannelli L, Reid PC, Stige LC, Stenseth LC (2009) Effects of environmental conditions on the seasonal distribution of phytoplankton biomass in the North Sea. *Limnol Oceanogr* 54(2): 512–524

Martinsen E, Engedahl H, Ottersen G, Ådlandsvik B, Loeng H, Balino B (1992) Metocean MOdeling Project, Climatological and hydrographical data for hindcast of ocean currents. *Tech. Rep. 100*, Norwegian Meteorological Institute, Oslo, Norway.

Melsom A, Fossum I (2009) Validation of an ocean model ensemble for the Barents Sea and the northeastern Nordic Seas. *met.no report 2/2009,* Norwegian Meteorological Institue, Oslo, Norway. ISSN: 1503-8025.

Melsom A, Gusdal Y (2009) A new method for assessing impacts of potential oil spills. *Proceedings from the 2008 EUROGOOS conference*. Submitted. 4 pp.

Neuwirth E (2007) RColorBrewer: ColorBrewer palettes. R-package version 1.0-1 .Available from: http://www.personal.psu.edu/cab38/ColorBrewer/ColorBrewer_intro.html.

Ottersen G, Helle K, Bogstad B (2002) Do abiotic mechanisms determine interannual variability in length-at-age of juvenile Arcto-Norwegian cod? *Can J Fish Aquat Sci* 59: 57-65.

Ottersen G, Stenseth NC (2001) Atlantic climate governs oceanographic and ecological variability in the Barents Sea. *Limnol Oceanogr* 46(7): 1774–1780.

Planque B, Bellier E, Lazure P (2007) Modelling potential spawning habitat of sardine (*Sardina pilchardus*) and anchovy (*Engraulis encrasicolus*) in the Bay of Biscay. *Fish Ocenogr* 16 (1): 16-30.

R development core team (2007) R: A language and environment for statistical computing.R Foundation for Statistical Computing. Available from: http://www.R-project.org.

Raknes A, Sunnanå K (1986) Acoustic estimates of spawning cod off Lofoten in 1986. *ICES C.M.* 1986/G:79.

Røed L, Debernard J (2004) Description of an integrated flux and sea-ice model suitable for coupling to an ocean and atmosphere model. *met.no Report 4/2004*, Norwegian Meteorological Institute, Oslo, Norway.

Saborido-Rey F, Kjesbu OS, Thorsen A (2003) Buoyancy of Atlantic cod larvae in relation to developmental stage and maternal influences. *J Plank Res* 25 (3): 291-307.

Skarðhamar J, Slagstad D, Edvardsen A (2007) Plankton distributions related to hydrography and circulation dynamics on a narrow continental shelf off Northern Norway. *Estuarine Coastal Shelf Sci* 75: 381-392.

Sundby S, Nakken O (2008) Spatial shifts in spawning habitats of Arcto-Norwegian cod

related to multidecadal climate oscillations and climate change. *ICES J Mar Sci* 65:953–962.

Vikebø F, Sundby S, Ådlandsvik B, Fiksen Ø (2005) The combined effect of transport and temperature on distribution and growth of larvae and pelagic juveniles of Arcto-Norwegian cod. *ICES J Mar Sci* 62:1375–1386.

Vikebø F, Jørgensen C, Kristiansen T, Fiksen Ø (2007) Drift, growth, and survival of larval Northeast Arctic cod with simple rules of behaviour. *Mar Ecol Prog Ser* 347: 207–219.

Wood SN (2003) Thin plate regression splines. *J Roy Stat Soc B* 65:95–114.

Wood SN (2004) Stable and efficient multiple smoothing parameter estimation for generalized additive models. *J Am Stat Assoc* 99:637–686.

Wood SN (2006) Generalized additive models: An introduction with R. Chapman and Hall/CRC.

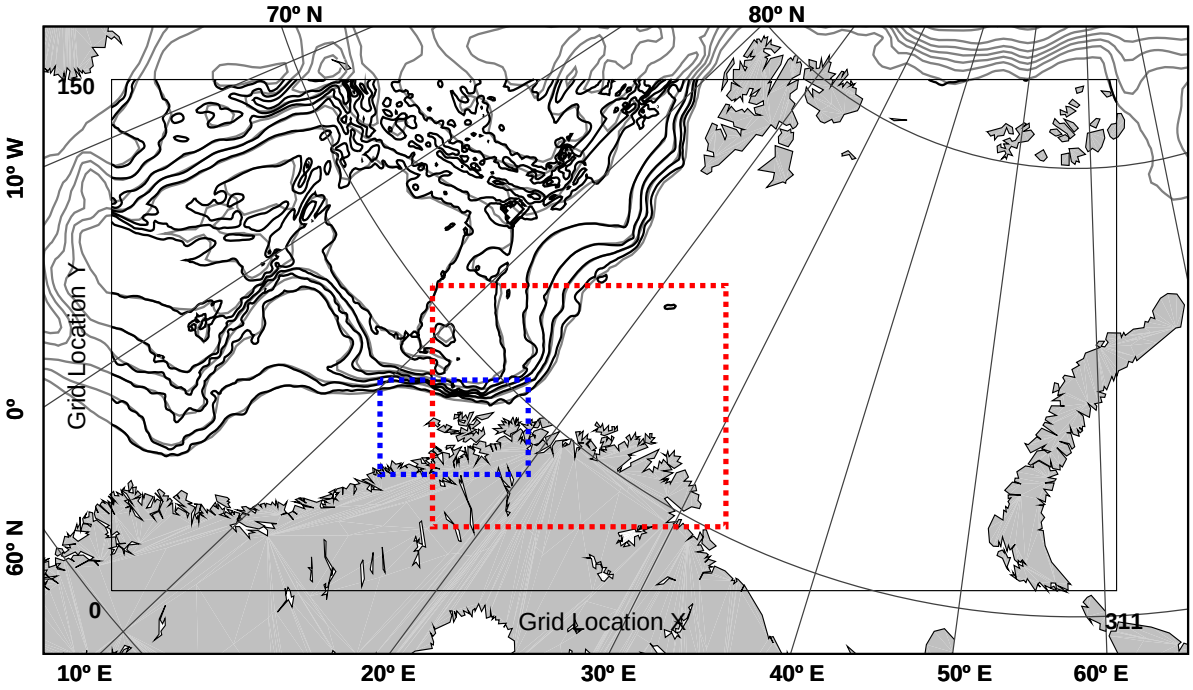

Figure 1. The Barents Sea-Lofoten ecosystem. The black outlined area square refers to the model area. Grey contours give the isobaths for the coarse model with a mesh size of 20 km; the isobaths for the fine mesh grid model (4 km) is marked with black isobaths. The contour interval for the topography is 500 m. The dotted blue line indicates the spawning area (Lofoten archipelago, Figure 2), and the dotted red line refers to the larvae area modeled (Figure 5).

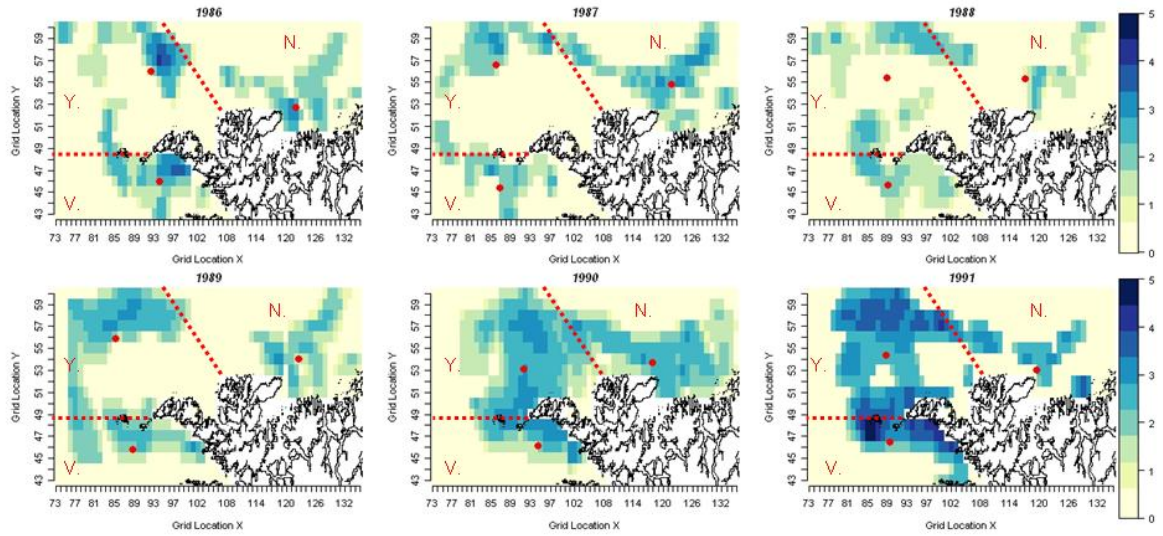

Figure 2. Relative cod spawners' abundance in the Lofoten archipelago for the six years of study. Units are expressed as log abundance of the acoustic survey data which is given as backscattering surface, square meter per nautical mile (m^2 / nm^2) (see *Materials and Methods* and Raknes and Sunnanå (1986) for details). Red dots represent the centre of gravity for each suarea (V., Vestfjorden, Y., Yttersida and N., Nord).

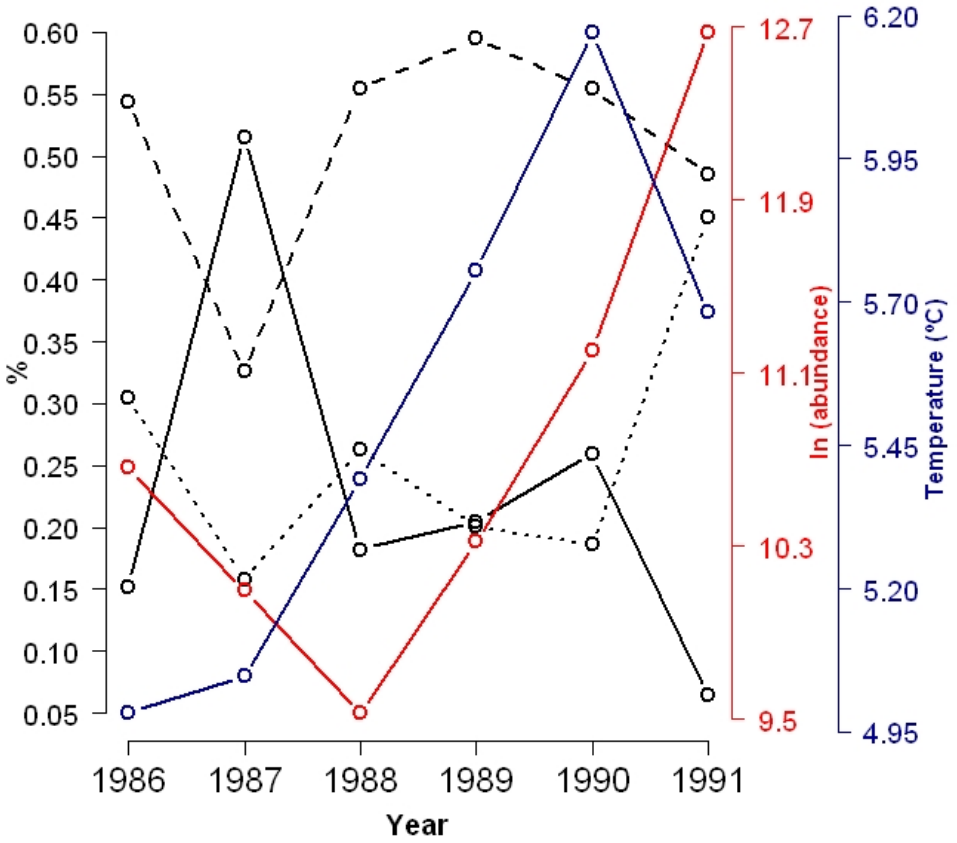

Figure 3. Percentage of spawners at each sub-area (Vestfjorden in dashed line, Yttersida in dotted line and Nord in solid line), log abundance of total spawners and mean sea temperature in upper water column (< 30 m) for March and April. Mean temperature was calculated averaging over the spawning area off Lofoten archipelago (Figure 2) one temperature distribution per week at 5 m, 10 m, 20 m and 30 m using values provided by the ocean/sea ice model (see *Material and Methods* for details).

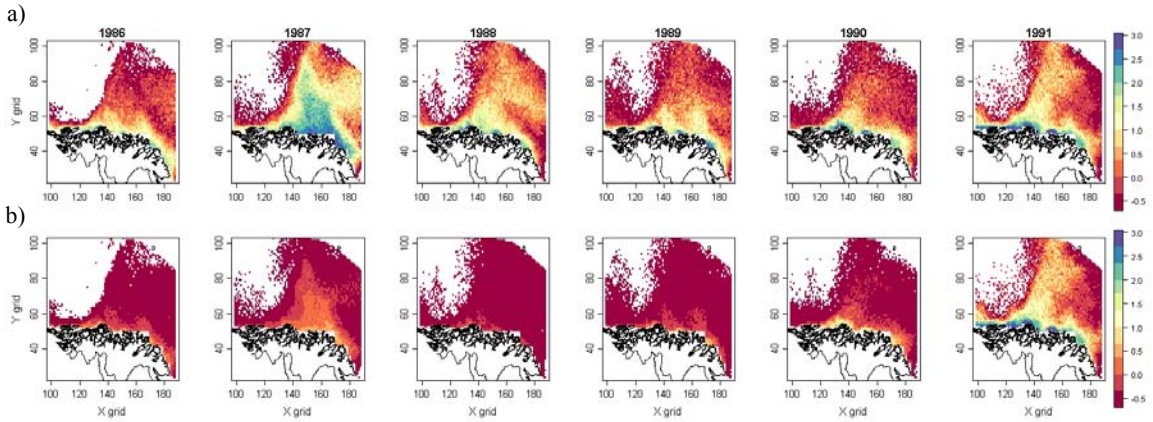

Figure 4. a) Distribution particles drifted (log[abundance]) for each year without taking into account interannual variation in spawners' abundance and distribution. b) Distribution particles drifted (log[abundance]) for each year taking into account interannual variation in spawners in each sub-area.

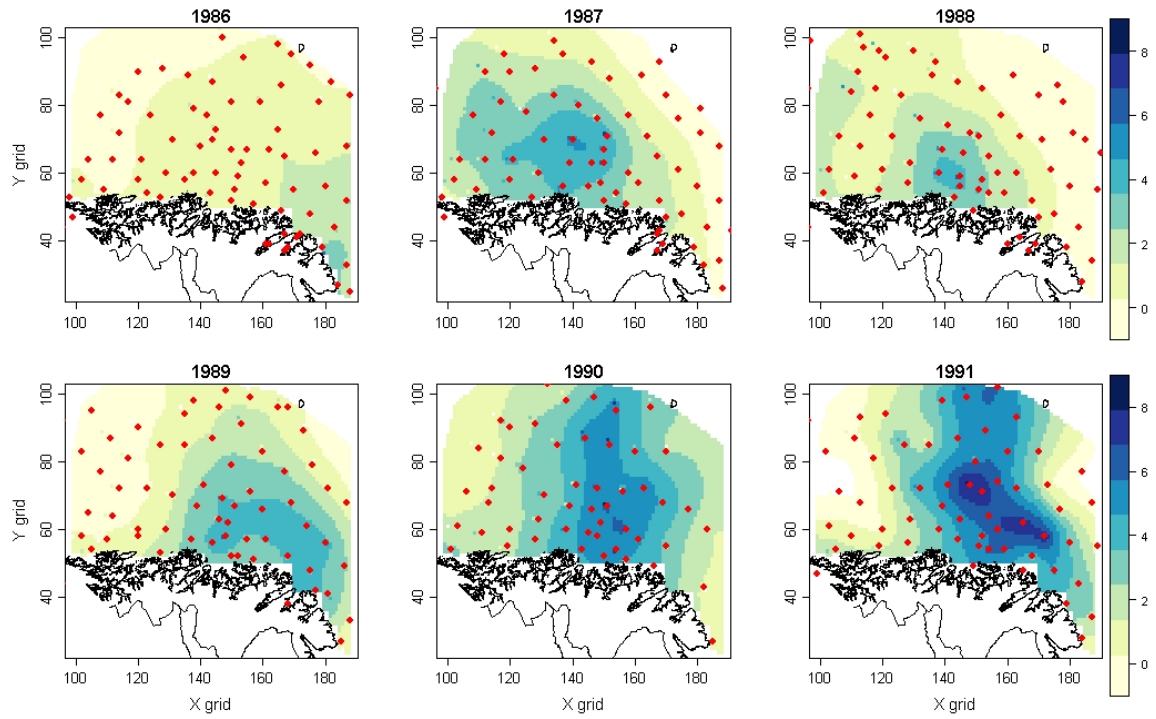

Figure 5. The distribution of larvae (log[abundance], smoothed using kriging) for each year. Red dots are the sampling locations.

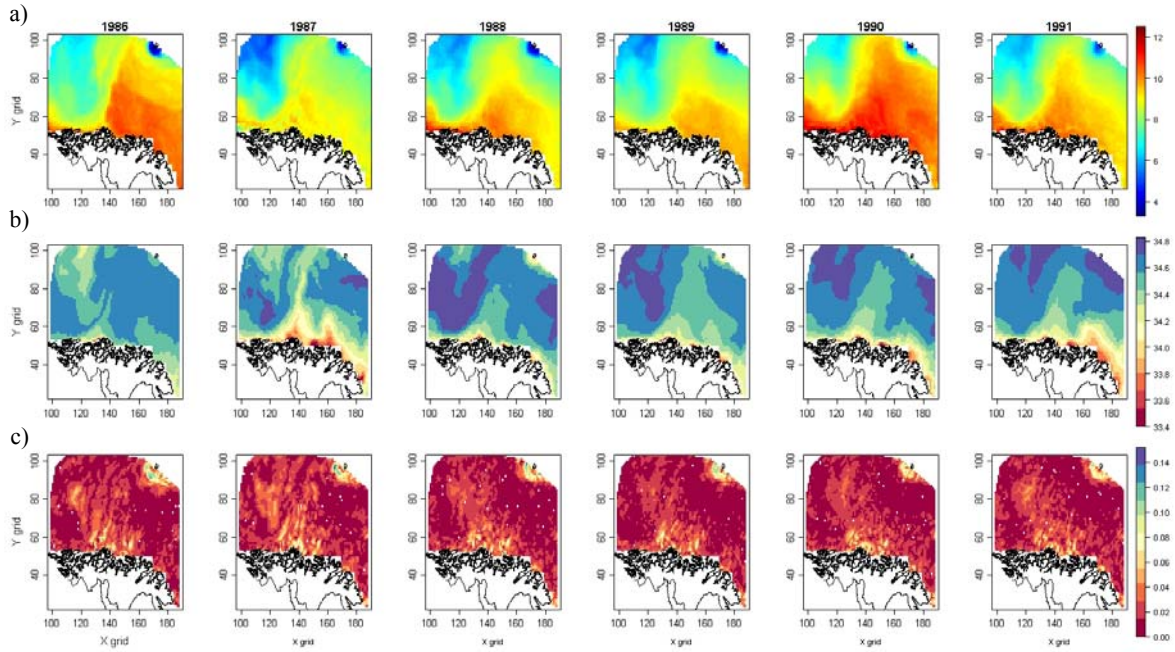

Figure 6. Annual seascape of the co-located environmental covariates calculated over two-week period (from June 24 to July 7) at 10 m depth and used in generalized additive modeling. a) Mean sea temperature, b) mean salinity and c) standard deviation of the convergence/divergence activity.

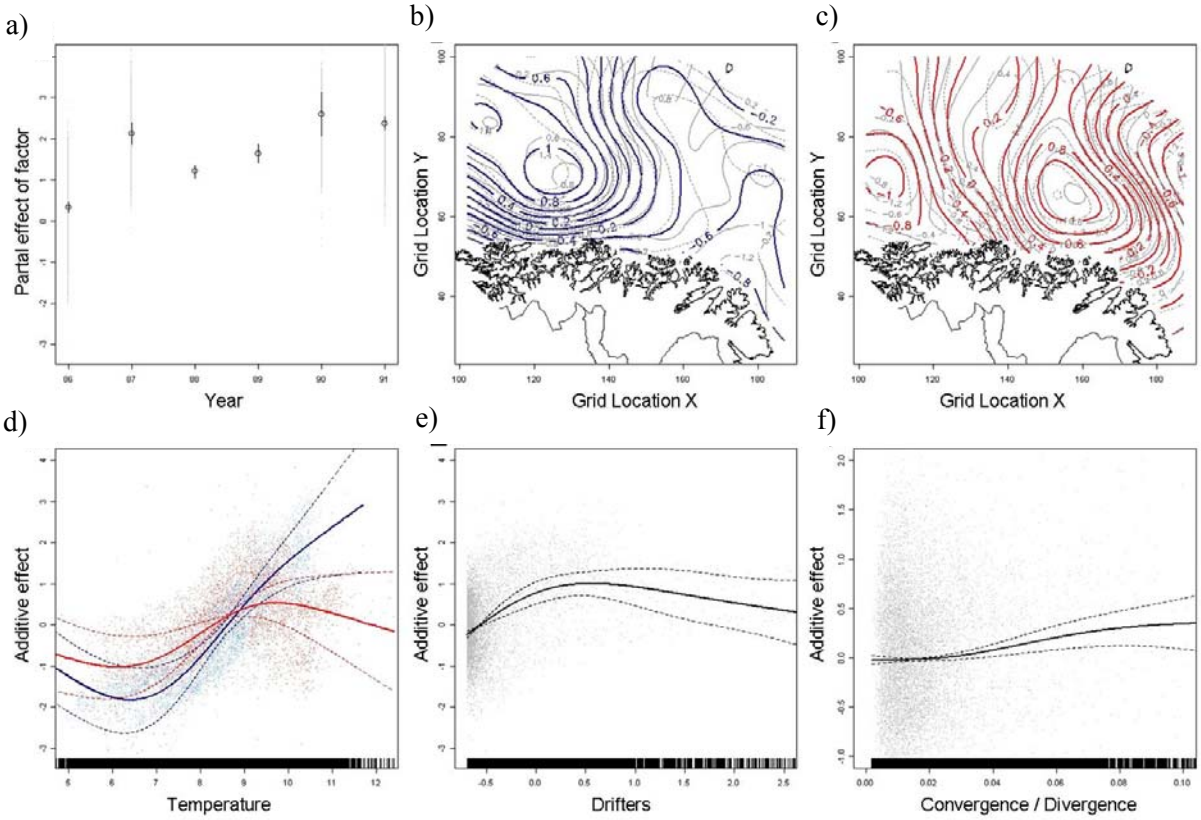

Figure 7. Results of the best model obtained, using threshold generalized additive modeling (TGAM). a) Year effect ($P < 0.05$). b) Spatial pattern for low NAO regime (<1, 1986-1988) ($P < 0.05$). c) Spatial pattern for high NAO regime (>1, 1989-1991) ($P < 0.05$). d) Temperature effect for low and high NAO regimes are represented in blue and red respectively (both additive effects $P < 0.05$). e) Drifters effect (density dependency) ($P < 0.05$). f) Convergence / divergence activity effect ($P = 0.073$). Whole and broken lines indicate fitted partial effects with 2*standard deviation from bootstrapping. Grey points represent the partial residuals for each smooth term. Note that the scale of the y-axis for convergence/divergence activity is different from the rest.

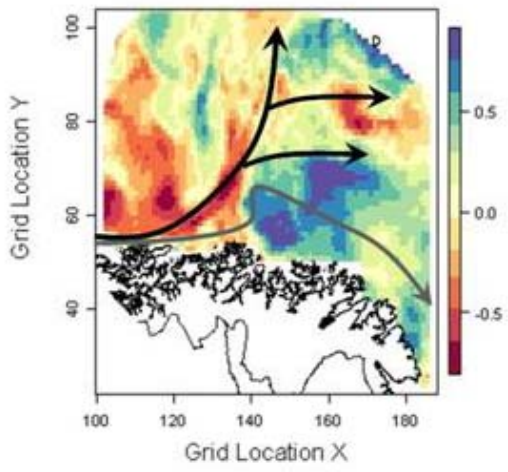

Figure 8. Correlation map between salinity and temperature showing the different water masses of the North Atlantic Current (NAC, black arrow) and Norwegian Coastal Current (NCC, grey arrow).